32nd URSI GASS, Montreal, 19-26 August 2017

Space Rubidium Clocks and the Light-Shift Effect

Valerio Formichella(1,2)
(1) Istituto Nazionale di Ricerca Metrologica, Strada delle Cacce 91, 10135 Torino, Italy
(2) Politecnico di Torino, Corso Duca degli Abruzzi, 10129 Torino, Italy

Abstract

Rubidium atomic frequency standards are currently the most common atomic clocks in global navigation satellite systems. Their frequency is affected by the light-shift effect due to the lamplight used for the optical pumping process, so that lamplight instabilities turn into frequency instabilities setting a limit to the navigation performance. Here we present the outcome of a study covering years of data from 10 GPS Rubidium clocks. We characterized the lamps' behavior; we found correlations between lamplight and frequency instabilities, like jumps and long-term variations, and used them to estimate the in-orbit light-shift coefficient. We found that the clock's long-term stability is limited by the lamp's one, and that the random walk frequency noise seems to be driven by a compound Poisson process by modelling lamplight jumps. Different solutions are proposed to overcome these problems and improve the performances of rubidium clocks and, thus, of global navigation satellite systems.

1. Introduction

Thanks to their low weight, small dimensions, low power consumption and high reliability, rubidium (Rb) atomic frequency standards (RAFS) are the most common atomic clocks used in global navigation satellite systems (GNSS) like GPS, Galileo and BeiDou. Their frequency is affected by the light-shift effect (LSE), a shift in the nominal frequency of the clock due to the optical pumping light from the Rb lamp [1]. Therefore, any variation of the lamplight intensity and spectrum leads to a variation of the clock frequency: the clock stability depends on the lamplight stability, setting a limit to GNSS performance. This problem is well known [2] but, for the first time, we have been able to analyze years of data from actual in-orbit RAFS to study the effect, uncovering the impact of the lamp on the clocks' performances and providing a possible explanation for the random walk frequency noise (RWFN). Different solutions have been proposed to overcome these problems. Here, we propose an active compensation of lamplight-induced frequency variations, currently under investigation in our group.

The paper structure is as follows. Section 2 briefly introduces the RAFS and LSE physics. Section 3 presents the observed in-orbit lamplight behavior, distinguishing different kinds of lamplight intensity variations. In section 4 we correlate lamplight and frequency variations; we estimate the light-shift coefficient (LSC), and we show how the clock's long-term frequency stability is limited by the lamplight intensity stability. Section 5 gives a possible explanation to the RAFS RWFN as the result of a compound Poisson process that maps lamplight jumps into RAFS frequency jumps by the LSE. Section 6 lists some possible solutions to the RAFS LSE problem, with particular attention to a proposed active compensation of lamplight-induced frequency variations.

2. An Introduction to RAFS and LSE

2.1 RAFS

The typical structure of a RAFS is shown in Figure 1. The basic idea is to lock the frequency of a voltage-controlled crystal oscillator (VCXO), multiplied by a synthesizer, to the frequency of an atomic transition. In this case, the ^{87}Rb ground state hyperfine transition at 6834.7 MHz [3].

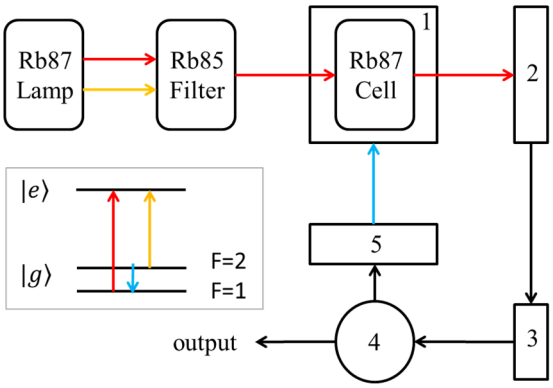

Figure 1. Structure of a RAFS. Besides the lamp and the filter and resonance cells, the other elements are: 1 the microwave cavity, 2 the photodetector, 3 the electronics controlling the VCXO (feedback), 4 the VCXO, and 5 the frequency synthesizer multiplying the VCXO's output up to the microwave regime.

An rf-discharge lamp produces Rb resonance. The light spectrum is shaped by passage through a filter cell, and then enters the resonance cell (sitting inside a microwave cavity), causing atoms to move from the F=1 to the F=2 level preparing them for the interrogation phase. During this phase, if the microwave frequency is tuned onto the hyperfine transition frequency, the population imbalance created by optical pumping is destroyed, with a decrease in light intensity reaching the photodetector (PD). Instead,

if the microwaves are not properly tuned, the F=1 level remains empty of atoms, and the resonance cell stays transparent to the light. The change in light intensity reaching the PD generates the feedback signal that locks the VCXO to the atoms' hyperfine transition frequency.

2.2 LSE

The LSE is the shift of an atomic transition frequency due to the interaction between atoms and light [4]. The atom is polarized by the light's electric field $\vec{E}$, and the induced dipole moment $\vec{p} \propto \vec{E}$ interacts with $\vec{E}$, yielding an energy perturbation of the atom:

$$\varepsilon = -\frac{1}{2}\vec{p}\cdot\vec{E} \propto \vec{E}\cdot\vec{E} \propto I \qquad (1)$$

where I is the light intensity. As suggested by (1), the shift of the energy levels and, therefore, of the transition frequencies is proportional to the light intensity. The proportionality coefficient $\alpha(\omega)$ depends on the light frequency ω, hence for a non-monochromatic light it is necessary to integrate over the whole spectrum. If $\Delta\nu_{LS}$ is the frequency shift and $S(\omega)$ the normalized spectral density, we have:

$$\Delta\nu_{LS} = \int \alpha(\omega)dI(\omega) = I\int \alpha(\omega)S(\omega)d\omega \equiv \beta I \qquad (2)$$

where I is the total light intensity and β is the LSC. The corresponding clock fractional frequency deviation is

$$y_{LS}(t) = \frac{\Delta\nu_{LS}(t)}{\nu_0} = \frac{\beta(t)I_0}{\nu_0}\frac{I(t)}{I_0} \equiv \kappa(t)i(t) \qquad (3)$$

where ν_0 is the nominal transition frequency, I_0 is the nominal lamplight intensity, $i(t)$ is the normalized intensity, and $\kappa(t)$ is the parameter usually reported as the clock's LSC [1]. Henceforth, i and κ will be referred to as the clock's lamplight and LSC, and κ will be considered constant in time. The total fractional frequency deviation of the clock will be

$$y(t) = y'(t) + y_{LS}(t) \qquad (4)$$

where y' indicates the contributions other than the LSE. Henceforth, y will be referred to as the clock's frequency.

3. In-Orbit Lamplight Behavior

We analyzed more than 10 years of lamplight data from a set of 10 GPS Block IIR in-orbit RAFS. Before analyzing them, we averaged the data over one-day non-overlapping batches. Detailed analysis can be found in [1, 5].

3.1 Deterministic Variations

The lamplight of the observed RAFS shows a long-term deterministic variation of the form

$$i(t) = Ae^{-t/\tau} + Bt + C \qquad (5)$$

with τ of the order of one year. Figure 2 provides an example with data from two different satellites.

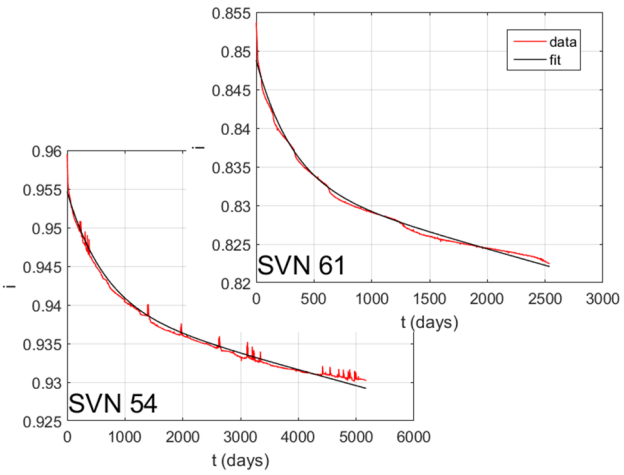

Figure 2. Lamplight data (red) from GPS satellites SVN 54 and 61. The black line is a fit with the model in (5).

3.2 Lamplight Jumps and Periodic Ramps

Some of the RAFS show clear lamplight jumps of at least two different types, i.e. step-like and spike-like jumps. Some examples are reported in Figure 3. Smaller and more numerous jumps can be found, depending on the actual jump definition [5] (see also section 5). Up to now, these are considered to be stochastic events with random occurrence, amplitude and duration. Another kind of observed instability is a periodic ramp of unpredictable duration and amplitude, also reported in Figure 3.

3.3 Non-stationary noise

Besides jumps and ramps, the RAFS' lamplight can show non-stationary noise superimposed on the deterministic variation. Figure 4 provides an example of a detrended lamplight data series with the corresponding stability, in terms of Allan deviation (ADEV). We do not comment on the white noise visible on the short term, which could be due to the measurement noise. Instead, we note that on the long term the lamplight stability seems to be affected by a random walk. We obtained similar results with longer data series from other satellites, and the results are reported in [1]. The estimated random walk contribution to the lamplight ADEV is $\sigma_y(\tau) = 5.1\times10^{-8}\,\tau^{1/2}$, with τ in seconds.

4. Lamplight/Frequency Correlation

In principle, any lamplight variation should translate into a frequency variation according to (3) and (4). The most evident correlation is the one between large lamplight and frequency jumps. For each lamplight-induced frequency jump, the LSC can be estimated as the ratio between the

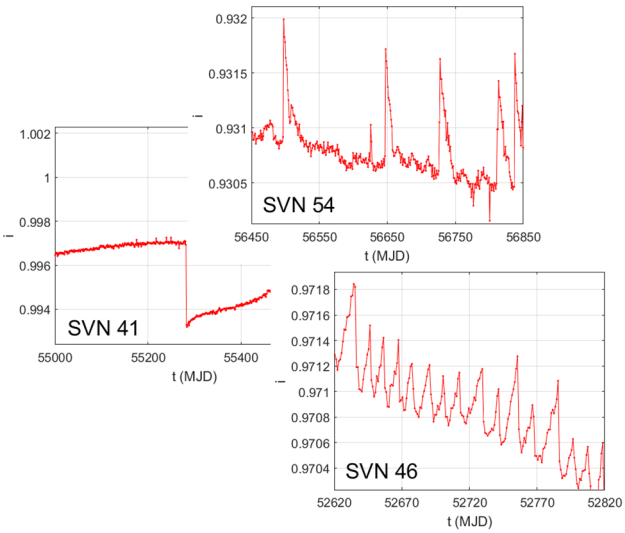

Figure 3. A step-like lamplight jump from GPS satellite SVN 41; some spike-like jumps from satellite SVN 54; periodic ramps from satellite SVN 46.

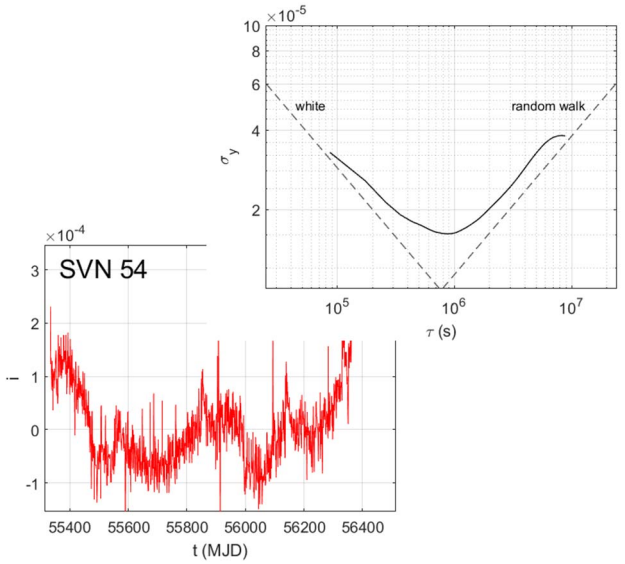

Figure 4. Detrended lamplight data (red) from GPS satellite SVN 54 and the corresponding ADEV, showing a random walk for averaging times τ larger than 10 days.

jumps' amplitudes: $\kappa = \Delta y/\Delta i$. It is more difficult to find a correlation between the deterministic lamplight and frequency variations, since the frequency could receive contributions different from the LSE, masking the true correlation. However, once potentially uncorrelated trends have been removed, one can look for correlations between residual fluctuations of the detrended data, i_D and y_D:

$$y_D(t) = \kappa i_D(t) + \text{noise}\,. \tag{6}$$

We compute the Pearson-product correlation coefficient r and, in case of good correlation ($r \geq 0.5$), we estimate κ as the slope of the regression line. Further details about these two methods for estimating κ can be found in [6].

Figure 5 shows some examples of correlated lamplight/frequency variations. See [1] for a collection of LSC estimates obtained from the observed RAFS. Their average is -1.9×10^{-10} with a standard deviation of 0.3×10^{-10}. Multiplying the random walk term of the lamplight ADEV by this LSC, we find a lamplight-inferred frequency ADEV, which is expected to be a lower limit for the long-term stability of the RAFS. With a 95% confidence interval for the LSC, this limit lies between $6.6 \times 10^{-18}\ \tau^{1/2}$ and $1.3 \times 10^{-17}\ \tau^{1/2}$. Such a result is validated by the manufacturer's data [7]. Actually, these numbers show that the lamplight-inferred random walk plays a fundamental role in the limitation of the GPS Block IIR RAFS long-term stability, which lies roughly between $1.5 \times 10^{-17}\ \tau^{1/2}$ and $1.5 \times 10^{-16}\ \tau^{1/2}$.

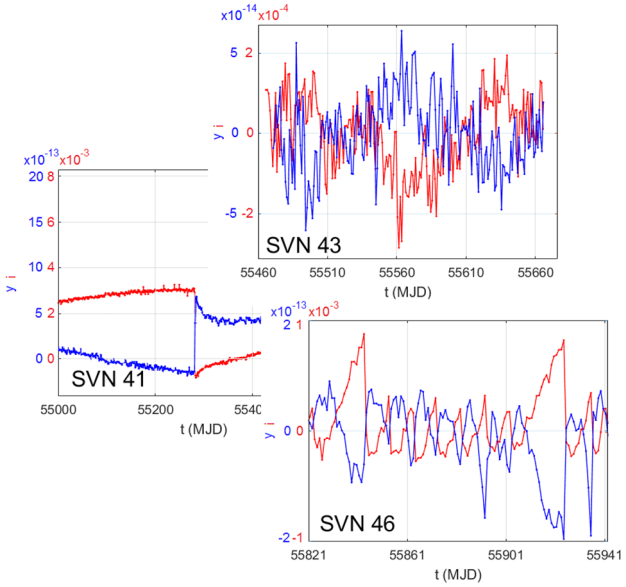

Figure 5. Correlated lamplight/frequency (red/blue) variations: a fast jump from GPS satellite SVN 41, long-term variations from SVN 43, ramps from SVN 46.

5. Lamplight Jumps and RAFS RWFN

In [5] we used the jump detector described in [8] to look for lamplight jumps within the available data series. Comparing each data point with a linear extrapolation based on the previous three points, we were able to find smaller and more numerous jumps. Collecting jumps statistics, in [9] we proposed a model for the lamplight jumps: a compound Poisson process with a mean waiting time between jumps of $1/\lambda$, where each jump has a random amplitude taken from a zero-mean Gaussian distribution with a clock-dependent standard deviation σ. In [10] we computed the analytical ADEV of a compound Poisson process: with a zero-mean jump amplitude, it is given by

$$\sigma_y(\tau) = \sqrt{\frac{\sigma^2 \lambda}{3}}\ \tau^{1/2} \tag{7}$$

which is the same as for a random walk (usually described by a Wiener process). Therefore, we made the hypothesis that the RAFS random walk could be caused by the lamplight jumps, via the LSE. We tested the hypothesis in [9], using the LSC estimated in [1] along with λ and σ estimated in [5], by simulating frequency fluctuations induced by a lamplight compound Poisson process. The results are reported in Figure 6, taken from [9], and show a good agreement between the simulated ADEV and the manufacturer's ADEV, corroborating our hypothesis.

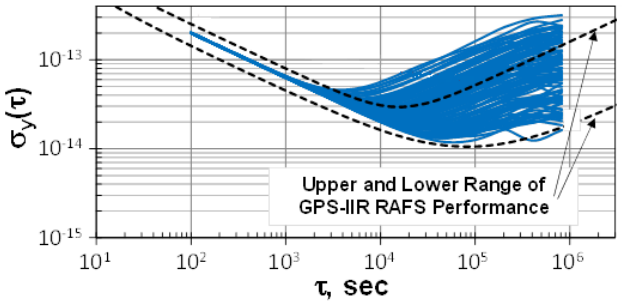

Figure 6. ADEV of 100 simulated RAFS with lamplight-induced frequency jumps (blue), covering the range measured on ground by the manufacturer (dashed curves).

6. Solving the LSE Problem

An obvious solution to the problem of lamplight-induced RAFS instabilities is to make the lamp quieter and/or the LSC smaller. The first objective cannot be achieved while the observed jumps and stochastic variations remain unexplained. Reducing the LSC could be possible acting on the filter and resonance cells, due to its dependence on the light spectrum and on the buffer gas pressure [11, 12]. Another solution is represented by the pulsed optically pumped Rb clock [12]. In this case, the optical pumping light is produced by a laser that is turned off during the interrogation phase, so that the hyperfine structure is not influenced by the LSE. Finally, we propose as a possible solution an active compensation of the lamplight-induced frequency variations, currently under investigation in our group. Briefly, the PD output is processed by an on-board software, averaging the lamplight data and scanning them with a suitable jump detector. The amplitude of any detected lamplight jump is multiplied by the LSC, to obtain the corresponding frequency jump amplitude, and a frequency correction is then applied to the clock outputs. Of course, the correction is an additional source of instability, but it should improve the long-term stability by mitigating the RWFN arising from the lamplight jumps. Moreover, the software could be tuned to detect a possible large lamplight jump with a time delay useful for navigation purposes. Indeed, after a large frequency jump, the information disseminated by the navigation message could be degraded: to avoid degradation of the navigation performance, the satellite could mark itself as "unusable" until the next message upgrade. However, if the jump is corrected before the next upgrade, the satellite returns to "usable" in a shorter time.

7. Acknowledgements

The author is really grateful to Dr. James Camparo and Dr. Patrizia Tavella for their invaluable work and help. Our collaboration involves several people from The Aerospace Corporation, INRiM and Politecnico di Torino.

8. References

1. V. Formichella, J. Camparo, I. Sesia, G. Signorile, L. Galleani, M. Huang, and P. Tavella, "The ac stark shift and space-borne rubidium atomic clocks," *J. Appl. Phys*., **120**, 194501 (2016).

2. C. H. Volk and R. P. Frueholz, "The role of long-term lamp fluctuations in the random walk of frequency behavior of the rubidium frequency standard: a case study," *J. Appl. Phys.*, **57** (1985), pp. 980-983.

3. J. Camparo, "The rubidium atomic clock and basic research," *Phys. Today*, **60**, 11 (2007), pp. 33-39.

4. B. S. Mathur, H. Tang, and W. Happer, "Light shifts in the alkali atoms," *Phys. Rev.*, **171**(1) (1968), pp. 11-19.

5. V. Formichella, J. Camparo, and P. Tavella, "On-Orbit GPS RAFS Lamplight Variations: Statistics of Lamplight Jumps," to appear in Proc. 2017 PTTI.

6. V. Formichella, J. Camparo, and P. Tavella, "Light-shift coefficient in GPS rubidium clocks: Estimation methods using lamplight/frequency correlations," in Proc. 2016 EFTF.

7. R. T. Dupuis, T. J. Lynch, and J. R. Vaccaro, "Rubidium frequency standard for the GPS IIF program and modifications for the RAFSMOD program," in Proc. 2008 IFCS, pp. 655-660.

8. L. Galleani and P. Tavella, "An algorithm for the detection of frequency jumps in space clocks," in Proc. 42nd PTTI, pp. 503-508.

9. V. Formichella, J. Camparo, and P. Tavella, "Influence of the ac-Stark Shift on GPS Atomic Clock Timekeeping," to appear in *Appl. Phys. Lett.*.

10. V. Formichella, "The Allan variance in the presence of a compound Poisson process modelling clock frequency jumps," *Metrologia*, **53** (2016), pp. 1346-1353.

11. J. Vanier, R. Kunski, P. Paulin, M. Tétu, and N. Cyr, "On the light shift in optical pumping of rubidium 87: The techniques of "separated" and "integrated" hyperfine filtering," *Can. J. Phys.*, **60**(10) (1982), pp. 1396-1403.

12. A. Godone, F. Levi, C. E. Calosso, and S. Micalizio, "High-performing vapor-cell frequency standards," *Riv. Nuovo Cimento*, **38**(3) (2015).